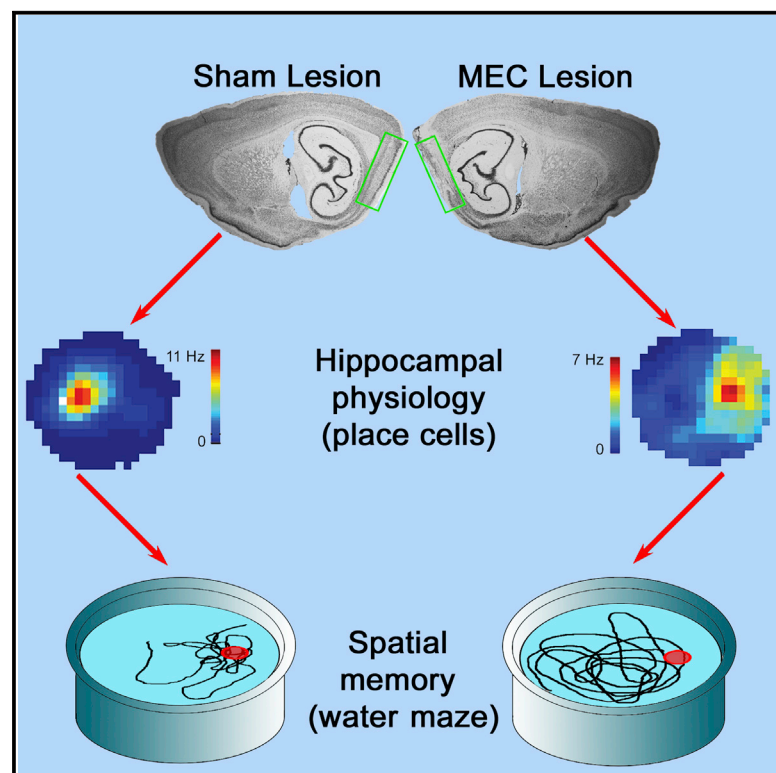# Medial Entorhinal Cortex Lesions Only Partially Disrupt Hippocampal Place Cells and Hippocampus-Dependent Place Memory

Graphical Abstract

Authors

Jena B. Hales, Magdalene I. Schlesiger, ..., Stefan Leutgeb, Robert E. Clark

Correspondence

sleutgeb@ucsd.edu (S.L.),
reclark@ucsd.edu (R.E.C.)

In Brief

To address whether the medial entorhinal cortex (MEC) is necessary for spatial coding and hippocampus-dependent memory, Hales et al. selectively removed the entire MEC in rats. This led to only partial deterioration of hippocampal spatial coding, and the MEC was found to be necessary for only a limited number of hippocampus-dependent memory tasks.

Highlights

Hippocampal place cells form without input from the medial entorhinal cortex

MEC lesions disrupt place cell precision and stability

MEC lesions impair a flexible type of place memory that involves navigation

MEC lesions spare other hippocampus-dependent spatial memory

Report

Medial Entorhinal Cortex Lesions Only Partially Disrupt Hippocampal Place Cells and Hippocampus-Dependent Place Memory

Jena B. Hales,[2,6] Magdalene I. Schlesiger,[4,6] Jill K. Leutgeb,[4] Larry R. Squire,[1,2,3] Stefan Leutgeb,[4,5,7,*] and Robert E. Clark[1,2,7,*]

[1]Veterans Affairs San Diego Healthcare System, San Diego, CA 92161, USA
[2]Department of Psychiatry, School of Medicine, University of California, San Diego, La Jolla, CA 92093, USA
[3]Department of Psychology and Department of Neurosciences, University of California, San Diego, La Jolla, CA 92093, USA
[4]Neurobiology Section and Center for Neural Circuits and Behavior, Division of Biological Sciences, University of California, San Diego, La Jolla, CA 92093, USA
[5]Kavli Institute for Brain and Mind, University of California, San Diego, La Jolla, CA 92093, USA
[6]Co-first author
[7]Co-senior author
*Correspondence: sleutgeb@ucsd.edu (S.L.), reclark@ucsd.edu (R.E.C.)
 http://dx.doi.org/10.1016/j.celrep.2014.10.009

SUMMARY

The entorhinal cortex provides the primary cortical projections to the hippocampus, a brain structure critical for memory. However, it remains unclear how the precise firing patterns of medial entorhinal cortex (MEC) cells influence hippocampal physiology and hippocampus-dependent behavior. We found that complete bilateral lesions of the MEC resulted in a lower proportion of active hippocampal cells. The remaining active cells had place fields, but with decreased spatial precision and decreased long-term spatial stability. In addition, MEC rats were as impaired in the water maze as hippocampus rats, while rats with combined MEC and hippocampal lesions had an even greater deficit. However, MEC rats were not impaired on other hippocampus-dependent tasks, including those in which an object location or context was remembered. Thus, the MEC is not necessary for all types of spatial coding or for all types of hippocampus-dependent memory, but it is necessary for the normal acquisition of place memory.

INTRODUCTION

Long-term memory for facts and events is thought to depend on the interaction of the hippocampus with widespread neocortical sites (McClelland et al., 1995; Squire and Alvarez, 1995). By virtue of its afferent and efferent connections, the entorhinal cortex connects between these regions. It provides the major cortical inputs to the hippocampus, receives backprojections from the hippocampus (Witter et al., 1989; Witter and Amaral, 1991), and has numerous connections to neocortical areas.

The projections from neocortical areas to the entorhinal cortex are segregated into two prominent streams, one through the medial entorhinal cortex (MEC) and a second through the lateral entorhinal cortex (LEC). The MEC is densely connected with the postrhinal cortex and is hypothesized to be specialized for representing spatial information, while the LEC is densely connected with the perirhinal cortex and is thought to be specialized for representing object information (Witter et al., 2000; Knierim et al., 2006; Eichenbaum et al., 2012). In support of this functional specialization, the MEC contains several cell types that are not found in the LEC. Most prominently, a substantial proportion of the principal cells in the MEC are grid cells, which fire at the vertices of highly regular triangular lattices (Hafting et al., 2005). Furthermore, within the MEC, grid cells are intermingled with other spatially and directionally modulated cell types such as head direction cells, conjunctive head direction-grid cells, border cells, and spatially periodic nongrid cells (Hafting et al., 2005; Sargolini et al., 2006; Solstad et al., 2008; Krupic et al., 2012). All of these cell types have been identified as projecting directly from the MEC to the dorsal hippocampus (Zhang et al., 2013) and are thought to be the primary source of spatial information for hippocampal place cells.

Given that MEC cells with spatial and directional firing patterns are a primary entorhinal input to the hippocampus, lesions of the MEC can be expected to markedly disrupt hippocampal spatial firing and spatial memory. It is therefore notable that prior lesion studies have often not reported marked effects on place cell physiology (Miller and Best, 1980; Van Cauter et al., 2008). In addition, memory impairment in hippocampus-dependent tasks after entorhinal lesions was found to be less robust than after hippocampal damage (Parron et al., 2004; Steffenach et al., 2005). A possible reason for mild impairments on spatial memory is that many of the reported entorhinal lesions may have spared the dorsocaudal-most part of the MEC, where the most precise spatial representations, including grid cells, are found.
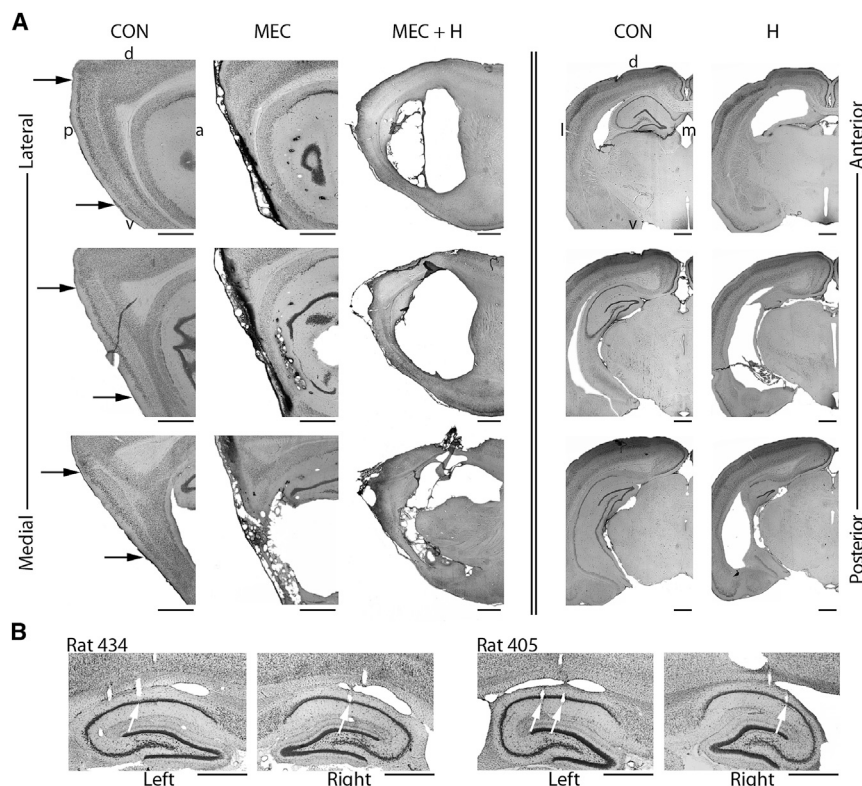
Figure 1. MEC Lesions and Hippocampal Lesions Included the Entire Dorsoventral Extent

(A) Photographs at three sagittal levels for rats with sham (CON), MEC, and MEC+H lesions (lateral to medial in the columns to the left of double line) and three coronal levels for rats with CON and H lesions (anterior to posterior in the columns to the right of double line). The letters around the two CON tissue sections in the top row identify the orientation of the sections (d, dorsal; v, ventral; a, anterior; p, posterior; l, lateral; m, medial). The black arrows in the left column indicate the dorsal and ventral borders of the MEC.

(B) Electrode tracks that terminated in the CA1 cell layer (marked by white arrows) in the left and right hemisphere are shown for two rats with MEC lesions.

See also Figure S1. Scale bars below each tissue section indicate 1 mm.

To determine whether spatial computations in the MEC support spatial memory, we developed a precise set of surgical coordinates for removing the entire MEC, including the most extreme portion of the dorsocaudal MEC. We then tested whether such complete lesions disrupted hippocampal spatial firing patterns. Next, we measured the effects of this MEC lesion on memory tasks, including the water maze, context and tone fear conditioning, and displaced and novel object recognition. For the water maze task, we also asked whether complete MEC lesions impaired performance as severely as full hippocampal lesions and whether combined MEC and hippocampal lesions produced a more severe impairment than separate lesions of each structure.

RESULTS

Medial Entorhinal Lesions Included the Grid Cell Area

To confirm that the entire MEC, including the dorsocaudal-most pole with a high proportion of grid cells, was included in the lesions, we determined the extent of entorhinal damage in sagittal sections (Figures 1 and S1). The sections were stained with NeuN to visualize any remaining neurons in the MEC, and the lesion extent was quantified using the Cavalieri method. In the MEC group, neurons were completely ablated in 82.6% of the total MEC volume (94.6% of layer II, 83.5% of layer III, and 75.2% of deep layers), with the majority of the sparing in the most lateral extent of the MEC. Cell loss in adjacent cortical areas was predominantly in the parasubiculum and postrhinal cortex and was minor in the ventral hippocampus and the LEC. In the group

with full hippocampal lesions (H), the damaged tissue included 74.4% of the total hippocampus, with the majority of the sparing at the most posterior transition between the dorsal and ventral hippocampus (coronal sections). In the group with combined H and MEC lesions (MEC+H), the lesion included 86.9% of the total hippocampus and 91.8% of the total MEC (95.1% of layer II, 91.3% of layer III, and 90.6% of deep layers).

A Subpopulation of Hippocampal Cells Remained Active but with Substantially Decreased Spatial Precision and Spatial Stability

To examine the extent to which hippocampal physiology was disrupted after the MEC lesion, we recorded hippocampal firing patterns while rats randomly foraged in familiar environments. First, we tested whether the substantial loss of inputs from the MEC to the hippocampus resulted in reduced hippocampal firing rates. The mean firing rate of all recorded cells during random foraging was 0.32 ± 0.04 Hz in the MEC group compared to 0.63 ± 0.09 Hz in the control (CON) group (mean $\pm$ SEM; $Z = 8.25$, p < 0.001) (Figure 2A). To test whether this difference in firing rate emerged from a higher proportion of cells that fired at extremely low rates during behavior, we selected cells that were active at average rates > 0.25 Hz during random foraging (90/198 [45.5%] in the MEC group and 67/107 [62.6%] in the CON group). The mean firing rate of this active cell population was 1.04 ± 0.09 Hz in the MEC group compared to 1.12 ± 0.12 Hz in the CON group (mean $\pm$ SEM; $Z = 0.01$, p = 0.99). Thus, even though there was a larger fraction of low-rate cells in MEC rats compared to controls, there was also a subpopulation of hippocampal cells in the MEC group that fired at control levels (Figure 2A).

The finding that a subpopulation of hippocampal cells continued to fire after the MEC lesion at rates that were comparable to those of place cells in CON rats raised the question
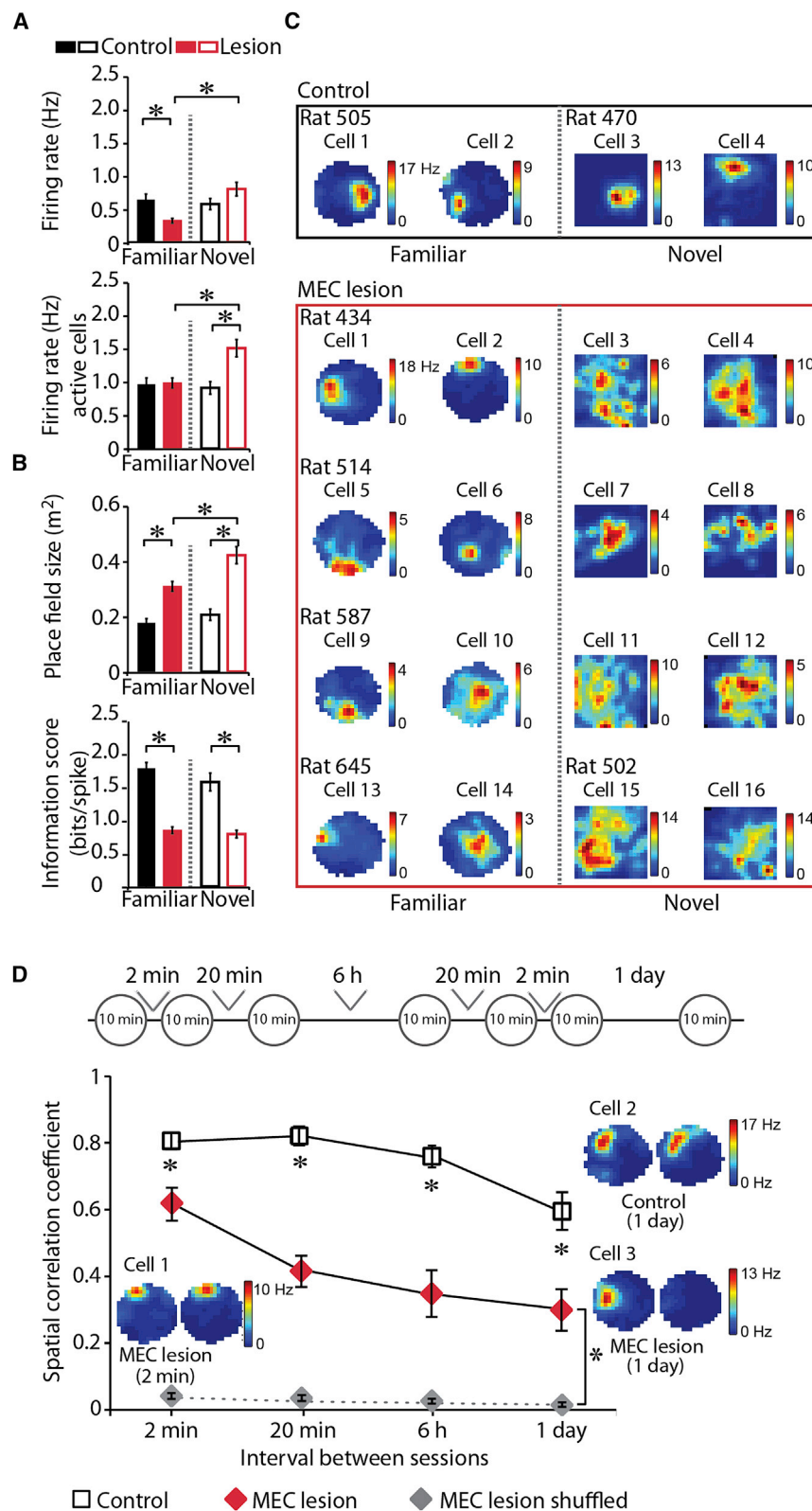
Figure 2. Neuronal Activity in the Hippocampus Was Disrupted after MEC Lesions

(A) Left: mean firing rate of all cells recorded during rest and/or random foraging in three daily 10 min sessions in a familiar environment (CON: black solid bar; n = 107 cells, n = 3 rats; MEC: red solid bar; n = 198 cells, n = 5 rats), and average neuronal firing rate in the population of cells that was active above a threshold of 0.25 Hz (active cells). Right: firing rates of all cells recorded in three 10 min sessions in the novel environment (CON: black open bar; n = 47 cells, n = 2 rats; MEC: red open bar; n = 118 cells, n = 4 rats) and of cells exceeding a mean firing rate threshold of 0.25 Hz.

(B) Differences in mean place field size and spatial information score between the CON and MEC groups indicate a substantial reduction in spatial precision after the MEC lesion, particularly in the novel environment. Only cells with mean firing rates > 0.25 Hz were included in the analysis.

(C) Spatial firing patterns of representative cells in the CON (black box) and MEC (red box) groups in the familiar (left) and novel (right) environment. The color scale for rate maps is from 0 Hz (blue) to peak rate (red).

(D) Place field stability was measured over a sequence of six 10 min foraging sessions in the familiar environment. To be included in the analysis, cells had to exceed a mean firing rate of 0.25 Hz in the first session of each comparison. Intervals between sessions were 2 min, 20 min, 6 hr, or 1 day (top schematic). The stability of spatial firing between sessions was lower in the MEC group compared to the CON group at all four tested intersession intervals as indicated by the lower mean spatial correlation coefficient (lower graph). However, the correlation values in the MEC group were higher than chance values that were calculated by shuffling the cell identity of active cells in the MEC group. Insets: spatial firing patterns of a representative control cell (1-day interval) and of two MEC lesion cells (2 min interval and 1-day interval) across two behavioral sessions.
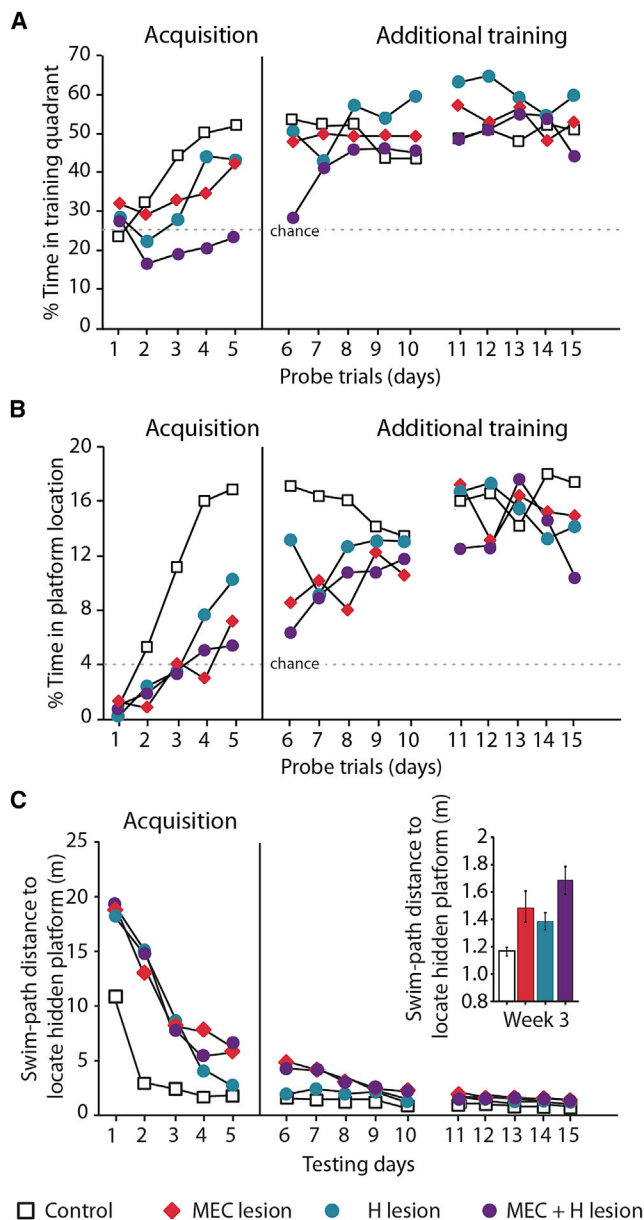
See also Figure S2. *p < 0.05. Error bars represent SEM.

Figure 3. Water Maze Performance Is Impaired after MEC, H, and MEC+H Lesions

Probe trial performance across the first 5 days of spatial memory acquisition (acquisition) and across ten additional training days (additional training) in rats with lesions of the hippocampus (H, n = 8), lesions of the medial entorhinal cortex (MEC, n = 8), lesions of both structures (MEC+H, n = 8), and sham lesions (CON, n = 20).

(A and B) The scores represent the percentage of time each group spent in the target quadrant (A) or in a small zone centered on the trained platform location (B) during a 60 s probe trial. Dashed lines indicate chance performance for the quadrant and small zone, which was 25% and 4%, respectively.

(C) All lesion groups were impaired at acquiring the platform location and required longer swim path distances than the CON group to locate the hidden platform. This impairment persisted throughout all 15 days of training. The inset bar graph is the average distance each group traveled to reach the platform during the third week of training. All three lesion groups took a longer average route to the platform than the

whether they might also have retained spatial selectivity. Hippocampal principal cells retained place-selective firing, but the firing fields of the cells in the MEC group were 94.4% broader, had 56.5% less spatial information, and were 23.9% less coherent than those in the CON group (place fields size: $Z = 6.02$, p < 0.001; spatial information: $Z = 7.98$, p < 0.001; spatial coherence: $Z = 6.58$, p < 0.001; Figures 2B, 2C, and S2). The decrease in the quality of spatial firing resulted in path reconstruction errors of 38.4 cm in ensembles of simultaneously recorded cells (n = 15–44 cells) from MEC rats compared to 22.7 cm in CON rats ($Z = 4.50$, p < 0.001; Figure S3A). In addition, the cells from MEC rats fired less consistently at the same location than those from CON rats over intersession intervals of 2 min, 20 min, 6 hr, or 1 day (Mann-Whitney U test, all p values < 0.01 after Holm-Bonferroni correction for multiple comparisons; Figure 2D). The most substantial decrease in place field stability was measured at the 1-day interval, but stability nonetheless remained higher than what would correspond to a random reorganization of place fields (Mann-Whitney test, $Z = 4.04$, p < 0.001).

After finding that spatial firing in the hippocampus was reduced in highly familiar environments after the MEC lesion, we tested the contribution of the MEC to the initial formation of hippocampal spatial maps. In contrast to the reduced firing rate in familiar rooms, hippocampal cells showed similar activity levels in a novel environment after MEC lesions (0.79 ± 0.10 Hz) compared to controls (0.57 ± 0.09 Hz, $Z = 0.23$, p = 0.41), and the proportion of active cells was similar to controls (69/118 [58.5%] in the MEC group and 29/47 [61.7%] in the CON group). In addition, cells active during random foraging (average firing rate > 0.25 Hz) fired at higher rates in MEC rats (1.50 ± 0.13 Hz) compared to CON rats (0.91 ± 0.09, $Z = 2.29$, p < 0.05). Along with the overall increase in neuronal activity in the novel environment, the firing fields in MEC-lesioned rats were broader than those in familiar environments. Hippocampal spatial firing patterns in MEC-lesioned rats were thus particularly disrupted when rats were first exposed to a novel environment.

MEC Lesions Impaired Spatial Memory in the Water Maze Task

The recordings from hippocampal place cells demonstrated that large MEC lesions substantially disrupted the precision and stability of hippocampal spatial firing, particularly in novel environments. Accordingly, we expected to find substantial deficits in spatial memory acquisition. To measure spatial memory performance after MEC lesions, we used a standard training protocol in the Morris water maze (four training trials per day) but with an added reinforced probe trial at the beginning of each training day to determine the learning rate. Rats with MEC lesions were profoundly impaired at acquiring memory for the platform location (repeated-measures ANOVA for group: $F_{(1)} = 18.74$, p < 0.001; Figure 3). With extended training, these rats eventually reached control performance levels for time spent in the target quadrant (after 5 days of training; Figure 3A) as well as for the

CON group (see Figure S3 and the Supplemental Results for additional statistics).
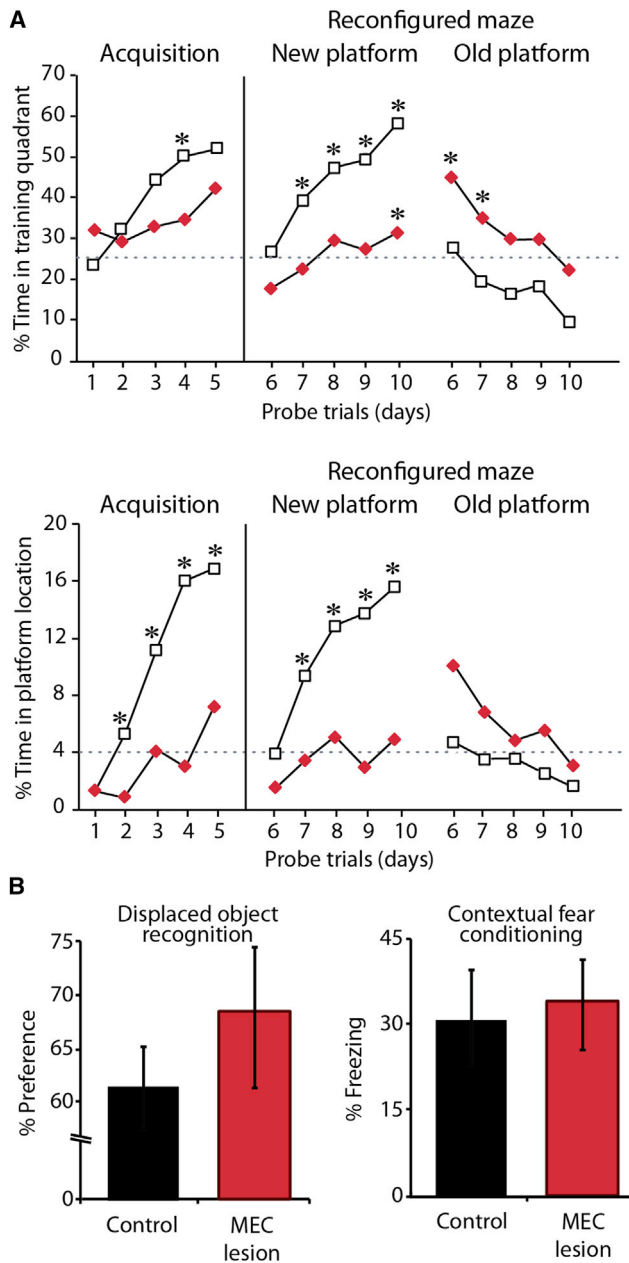Error bars represent SEM.

Figure 4. Water Maze Performance Is Inflexible after MEC Lesions despite Normal Performance on Other Tasks

(A) CON (n = 8) and MEC (n = 8) groups were given 5 days of initial water maze training. The water maze was then reconfigured by changing all the distal spatial cues, and the groups were trained for 5 additional days with the platform in the opposite quadrant (reconfigured maze). The scores to the left of the vertical line represent the percentage of time that each group spent in the quadrant containing the platform (top) or in a small circle centered on the platform (bottom) during initial training (acquisition). Scores to the right of the vertical line represent the performance of the groups in the reconfigured maze when the analysis was done with the new platform location (new platform) or with the old platform location (old platform). The MEC group was impaired on initial acquisition and in learning the new platform location in the reconfigured maze (new platform). Whereas the CON group approached the reconfigured maze as a new maze and never spent greater than chance amount of time at the old platform location, the MEC group persisted in

time spent in a small circle around the platform location (after 9 days of training; Figure 3B).

To determine whether MEC rats found an alternate strategy for solving the task, we tested spatial memory in the original and in a reconfigured water maze. A separate set of animals (MEC and CON groups) was trained for 5 days on the water maze as described above. During a second week, the groups were then tested in a reconfigured environment. The room and pool remained the same, but the distal visual cues and the platform location were changed. After reconfiguring the room, the CON rats performed as expected for a new maze, with chance levels of performance on the first day and rapid learning across the following 4 days (Figure 4A). In contrast, the memory deficit in the MEC group was so profound that they did not learn the new platform location, never performing above chance on the small circle measure (all t values < 1.04, $p > 0.1$) and performing above chance only on the fifth day for the quadrant measure ($t_{(7)} = 2.77$, $p < 0.05$). Instead of showing improvement for the new platform location, the MEC rats showed a strong preference for the old platform location, performing above chance at that location until day 3 by the quadrant measure (days 1 and 2: $t > 2.38$, $p < 0.05$). In summary, although the MEC rats eventually performed comparably to controls after extended training on the first platform location, their performance in a reconfigured maze was severely impaired compared to CON rats (all t values for the small circle and quadrant measures > 2.74, $p < 0.05$) indicating that they came to approach the task in a different way than CON rats and that their ability to rapidly and flexibly form new place memories was impaired.

Comparison of MEC Lesions to Hippocampal Lesions and to Combined MEC and Hippocampal Lesions

Once we determined that MEC rats were impaired at acquiring the water maze task but were eventually able to reach asymptotic levels with extended training, we asked whether the extent of the learning deficit after an MEC lesion might be comparable to that of a complete hippocampal lesion. H rats also eventually reached control performance levels for the quadrant measure (after 4 days of training; $t_{(26)} = 1.17$, $p > 0.1$; Figure 3A) as well as for the small circle measure (after 8 days of training; $t_{(26)} = 1.58$, $p > 0.1$; Figure 3B) and, similar to MEC rats, learned the platform location with extended training. In particular, the number of training days until each of the groups showed memory for the platform location was similar. Therefore, the performance of the H group was comparable to that of the MEC group (repeated-measures ANOVA for group: $F_{(1)} = 0.17$, $p > 0.1$).

The similar effects of MEC and H lesions on spatial memory could indicate that a lesion of either area fully disrupted the

searching for the platform in the old location (old platform). Dashed line represents chance performance on a 60 s probe trial.

(B) Performance of the CON (n = 8) and MEC (n = 8) groups on two hippocampus-dependent memory tasks requiring spatial information. Both groups preformed equally and above chance on displaced object recognition (left) and on context memory as measured by percent freezing (right). Both groups also performed equally and better than chance on the novel object recognition task and freezing to a tone paired with shock (data not shown).

*$p < 0.05$. Error bars represent SEM.

function of the entorhino-hippocampal loop and that the residual capacity for learning was supported by different brain areas. Alternatively, the similar effects could indicate that in each case the intact brain area (hippocampus or MEC) can support some spatial learning. To examine whether the MEC and hippocampus can independently support spatial memory function, we compared the MEC and H groups to rats with a combined lesion of the MEC and hippocampus. For the quadrant measure, the MEC+H group had a much more pronounced deficit than either the MEC or H group (through day 6; MEC+H relative to MEC: $t_{(14)} = 2.99$, p < 0.01; MEC+H relative to H: $t_{(14)} = 2.71$, p < 0.05; Figure 3A). A comparison of the rate of memory acquisition showed that CON rats performed above chance levels beginning on day 2 of acquisition ($t_{(19)} = 4.75$, p < 0.001), and H and MEC rats performed above chance levels on days 4 and 5, respectively (H: $t_{(7)} = 3.48$, p < 0.05; MEC: $t_{(7)} = 2.88$, p < 0.05). In contrast, MEC+H rats failed to perform above chance until day 8 ($t_{(7)} = 4.39$, p < 0.01). By the third week of testing, there were no longer significant group differences (repeated-measures ANOVA for group: $F_{(3)} = 1.53$, p > 0.1). All lesion groups were also impaired at finding the platform during the acquisition training trials (repeated-measures ANOVA for group: $F_{(3)} = 10.57$, p < 0.0001). However, in contrast to the probe measures, all three lesion groups remained impaired through the end of the 15 days of training (Figure 3C; see the Supplemental Results for additional water maze results and statistics).

The substantial decrease in the precision of hippocampal spatial firing after MEC lesions (see Figure 2) might suggest that memory for a precise spatial location is more severely impaired after the MEC lesion compared to memory for broader locations. We examined this possibility by measuring the amount of time that rats spent directly at the platform location (i.e., the small circle measure). During the probe trials, the impairments of the MEC group and the H group were as severe as that of the combined MEC+H group. The H group reached control level performance at day 8, while the MEC and MEC+H groups reached control level performance on day 9 (Figure 3B). The CON group was already above chance levels beginning on day 3 of acquisition ($t_{(18)} = 5.62$, p < 0.001). By the third week, there were no longer significant group differences (repeated-measures ANOVA for group: $F_{(3)} = 0.47$, p > 0.1). Our results therefore indicate that the degree to which the MEC and hippocampus can independently support spatial memory depends on the spatial precision that needs to be demonstrated (see the Supplemental Results and Figure S3 for additional water maze results).

Intact Performance after MEC Lesions on Other Memory Tasks

After finding a substantial memory deficit in the water maze, we tested the MEC and CON groups on a series of nonnavigational tasks that are sensitive to hippocampal damage. First, we examined displaced object recognition, which requires animals to preferentially explore a displaced object after a 3 hr delay. Preference for the displaced object did not differ between the MEC and CON groups (Figure 4B; $t_{(14)} = 0.92$, p > 0.1) and was above 50% chance in both groups (MEC: $t_{(7)} = 3.05$, p < 0.05; CON: $t_{(7)} = 2.27$, p = 0.058). As a nonspatial comparison, we asked whether novel object recognition, which requires rats to recognize a pre-

viously encountered object, is affected by an MEC lesion. Preference for the novel object did not differ between the MEC and CON groups ($t_{(14)} = 0.41$, p > 0.1) and was above 50% chance in both groups (MEC: $t_{(7)} = 6.23$, p < 0.0001; CON: $t_{(7)} = 5.25$, p < 0.0001). Next, we trained animals in context fear conditioning to associate a context (i.e., spatial environment) with a foot shock. For comparison, we also tested for fear conditioning to a tone paired with a shock (delay conditioning). The amount of freezing (i.e., the index of fear) did not differ between the MEC and CON groups on the test for context (Figure 4B; $t_{(14)} = 0.26$, p > 0.1) or on the test for the tone ($t_{(14)} = 0.22$, p > 0.1; see the Supplemental Results for additional context fear conditioning results). The amount of freezing in the context that was not associated with the shock also did not differ between the MEC and CON groups ($t_{(14)} = 0.48$, p > 0.1), suggesting that generalized fear did not support the spared function measured in the context associated with the shock. In summary, MEC rats were not impaired on any of the additional tasks including two standard hippocampus-dependent tasks that required an object location (i.e., displaced object recognition) or a spatial context to be remembered (i.e., context fear conditioning).

DISCUSSION

The majority of spatial and directional input to the hippocampus originates from specialized cell types in the MEC, such as grid cells, head direction cells, conjunctive head-direction-by-grid cells, border cells, and spatially periodic nongrid cells (Hafting et al., 2005; Sargolini et al., 2006; Solstad et al., 2008; Krupic et al., 2012; Zhang et al., 2013). Selective damage of the MEC could thus be expected to result in a substantial disruption of hippocampal spatial firing and of hippocampus-dependent spatial memory. We produced nearly complete lesions of the MEC and found that the lesion broadened hippocampal place fields but did not completely prevent their formation. Such substantial disruption of hippocampal spatial firing patterns after MEC lesions would predict a major effect on hippocampus-dependent spatial memory. Although we observed memory deficits in the water maze that were equally severe as those after hippocampal lesions, we also found that hippocampus-dependent memory tasks that require memory for either an object location or a context were entirely unaffected by the MEC lesion as were two other nonspatial memory tasks (novel object recognition and tone fear memory).

The marked effect of our MEC lesion on hippocampal physiology and on spatial memory in the water maze differs from more subtle effects in prior studies that targeted the entorhinal cortex. Our lesion approach differed in that we excluded the LEC, but we made certain to include the most dorsocaudal MEC (dMEC), where the spatial firing of grid cells is most precise (Hafting et al., 2005). In recording studies that spared this region, hippocampal place fields became smaller (Van Cauter et al., 2008) or moderately larger (Brun et al., 2008) compared to controls. In another study in which the lesion extent within entorhinal cortex (EC) was large, but not particularly targeted to dMEC, there were no apparent effects on place field size (Miller and Best, 1980). The present lesions are the first where damage to the MEC was sufficient to result in a substantial increase in place

field size. However, even the most extensive MEC lesions did not completely disrupt hippocampal spatial firing.

In parallel with the previously reported mild effect of EC lesions on hippocampal physiology, the behavioral effects of EC lesions, including effects on water maze performance, have also generally been mild and smaller than effects after complete hippocampal lesions (Parron et al., 2004; Steffenach et al., 2005; although a more substantial water maze acquisition impairment has been reported in mice with a genetic disruption of the MEC; Yasuda and Mayford, 2006). We directly compared the behavioral effect of our MEC lesion with an essentially complete hippocampal lesion and found that the impairments in the water maze were equivalent. Although the effects of MEC and hippocampal lesions on spatial memory were severe, we also observed that the platform location was eventually learned in both lesion groups. To determine whether the spared performance depended on a different strategy for reaching the platform location in MEC rats, we tested rats on a reconfigured water maze and found that whereas the control rats rapidly learned a second platform location, MEC rats did not learn the second platform location and perseverated in searching at the old platform location. Thus, MEC lesions disrupted the ability to rapidly and flexibly form new spatial memories.

The residual capacity for inflexible spatial learning that we observed could be supported by spared processing within the entorhino-hippocampal loop. That is, the hippocampus might continue to process information through LEC inputs, or, after hippocampal lesion, the MEC might perform computations without receiving feedback from the hippocampus. For example, rats with hippocampal lesions have previously been shown to reach control levels of performance when they are overtrained in the water maze (Morris et al., 1990). Alternatively, the residual spatial learning could be entirely supported by brain regions outside of the MEC and hippocampus. To distinguish between these possibilities, we compared a lesion of the MEC or hippocampus alone to a combined lesion of both brain areas. We found that the impairment of the MEC+H rats was equivalent to the MEC or the H rats based on the time in the small target circle but was more severe in the combined lesion group compared to both single lesion groups based on the time in the target quadrant. Thus, our data show compensation for remembering the approximate, but not the precise, platform location, which might be supported by the broad residual firing patterns of MEC cells after hippocampal lesions (Fyhn et al., 2004) and of hippocampal cells after MEC lesions. It has been shown that spatial reference memory is retained while hippocampal maps reorganize (Jeffery et al., 2003), and our data after MEC lesions suggest that reference memory can also be supported when hippocampal firing patterns are only weakly stable. With further overtraining, compensation for remembering the precise platform location can occur even when both the hippocampus and the entorhinal cortex are damaged. Gradually acquired, inflexible navigation can thus be executed entirely without the spatial firing patterns in the hippocampus and MEC.

The input streams from the MEC to the hippocampus are predominantly spatial, and the streams from the LEC are predominantly nonspatial (Hargreaves et al., 2005; Knierim et al., 2006; Eichenbaum et al., 2012). We therefore expected that MEC lesions would impair most hippocampus-dependent tasks that require the rapid acquisition of spatial and contextual knowledge, including displaced object recognition (Mumby et al., 2002) and context fear conditioning (see Sanders and Fanselow [2003] for review). Similar to those studies, Van Cauter et al. (2013) used a one-trial recognition task where rats explored one object during a familiarization phase. During the test phase, presented 15 min later, an identical object was added to the arena. Control rats preferentially explored this object relative to the object from the familiarization phase that remained in place. MEC-lesioned rats failed to show this preference. In contrast, we found that the performance of MEC rats was intact on the displaced object recognition task; however, there were some key differences between our studies. Our version of the task was more difficult, because both objects were present during the familiarization phase and then one of those objects was displaced during the test phase. Further, we used a 3 hr delay and our lesions included more of the MEC than the Van Cauter et al. (2013) study reported. All of these factors should have made it more likely to observe an impairment in our study. Yet, our MEC group performed above chance and equal to controls. This spared performance can be explained in at least two different ways. (1) In spontaneous preference tasks, above chance performance is a strong indication of memory and perceptual ability. However, a failure to observe a significant preference, as was the case in the Van Cauter et al. (2013) study, does not necessarily mean a failure of memory or perception, but could be due to nonspecific factors like changes in exploratory behavior or motivation in the lesion group. (2) Comparing these two studies is further complicated by the fact that Van Cauter et al. (2013) used radiofrequency lesions, which damaged both cell bodies and fibers and could thus potentially extend to projections from the LEC. In contrast, we used excitotoxic lesions, which damaged only cell bodies in the MEC but spared fibers. It is possible that the performance was spared because spatial information from the LEC would still be available to the hippocampus. In support of this interpretation, physiological recordings from the LEC have shown some stable spatial selectivity relative to objects or previously encountered objects in an environment (Deshmukh and Knierim, 2011; Deshmukh et al., 2012; Tsao et al., 2013). Furthermore, a recent study showed that rats with LEC lesions had intact performance on the water maze but were impaired on a displaced object recognition task, suggesting that the LEC is necessary to detect differences in object configuration (Van Cauter et al., 2013), but not for remembering a consistent goal location.

We found that depriving the hippocampus of the rich spatial processing input stream from the MEC disrupted hippocampal place field precision and stability and impaired the ability to rapidly acquire the information needed to successfully perform in the water maze. In contrast, the MEC is not required to successfully recognize a context, detect a spatial change, associate a tone and shock, or recognize an object. Other work suggests that this area is critical for performance on nonspatial tasks that require the flexible use of memory (Sauvage et al., 2010; Navawongse and Eichenbaum, 2013). Thus, the MEC is not specialized for all forms of hippocampus-dependent memory but does appear critical for a limited range of tasks, including normal acquisition and use of place memory.

EXPERIMENTAL PROCEDURES

Subjects

The subjects were 84 experimentally naive, male Long-Evans rats. Groups with lesions of the MEC (n = 8), lesions of the hippocampus (H, n = 8), combined lesions (MEC+H, n = 8), and sham lesions (CON, n = 20) were tested in the water maze for 3 weeks. Additional rats (MEC, n = 8; CON, n = 8) were tested in the original water maze task for 1 week and in a reconfigured maze for a second week. These 16 rats were also tested on displaced and novel object recognition and on context and tone fear conditioning. Finally, one naive group (n = 16) was used as an unshocked fear conditioning control group. For all behavioral testing, rats were housed individually on a 12 hr light/dark cycle with continuous access to food and water. Testing was performed in the light phase. Eight additional rats underwent either MEC-lesion or sham surgery and were implanted with recording electrodes aimed bilaterally at the hippocampus (MEC, n = 5 and CON, n = 3). These rats were housed individually on a 12 hr reversed light/dark cycle, and the rats were food restricted and maintained at ∼90% of free-feeding body weight. Testing was performed in the dark phase. All procedures were in accordance with animal protocols that were approved by the University of California, San Diego Institutional Animal Care and Use Committee.

Surgery

All stereotaxic surgery was performed using isoflurane gas anesthesia. Lesions were produced by ibotenic acid in the hippocampus and by NMDA in the MEC. For hippocampal recordings, an electrode assembly was implanted during the same surgery as the MEC-lesion procedures (Koenig et al., 2011). The 14 tetrodes of the electrode assembly were arranged into two bundles, each aimed at one hemisphere and containing six to eight independently movable tetrodes. One electrode in each hemisphere was used to record a reference signal.

Electrophysiological Recordings

Rats were pretrained for 5 days in two 10 min sessions per day to forage for randomly scattered cereal crumbs. After surgery, tetrodes were slowly advanced into the CA1 area of the hippocampus, and training continued for 7–10 days with up to six 10 min sessions per day in a different room than during pretraining. Recordings during random foraging began when tetrodes were positioned in the CA1 cell layer and when the rats ran continuously over the entire box surface throughout each 10 min random foraging session. In addition to performing recording sessions in rooms in which the rats had been previously been trained, we also performed a series of three 10 min recording sessions in a novel room. See the Supplemental Experimental Procedures for additional detail on the electrophysiological recording and analysis methods.

Behavioral Testing

All behavioral testing was postoperative. See the Supplemental Experimental Procedures for additional detail on the behavioral testing methods.

Morris Water Maze

Each day, rats were given a reinforced probe trial followed by four standard training trials (Broadbent et al., 2004; Clark et al., 2005). Performance on the probe trial was calculated by measuring the percentage of time rats spent in the quadrant of the pool where the platform had been located during training (chance = 25%). In addition, we calculated the percentage of time each rat spent in a circular zone (30 cm diameter) centered on the point where the platform had been located during training (chance = 4%). During the remaining four standard training trials, the platform remained in its raised position. Rats were tested for 15 days.

Reconfigured Maze Protocol. An MEC group and a CON group were trained on the water maze task for 5 days as described above for week 1. In week 2, they were then given an additional 5 acquisition days in a reconfigured room. During this phase, the pool and room were the same as during week 1, but a curtain was hung around the pool, new distal visual cues were displayed on the curtain, and the platform location was moved to the opposite quadrant.

Displaced Object Recognition

Identical brown opaque plastic jars served as stimuli. During a 15 min familiarization phase, two jars were located in adjacent quadrants while the rat was allowed to explore the jars. Following a 3 hr delay, the rat was placed back into the apparatus for the test phase with one of the two jars relocated to a different quadrant. Spatial recognition memory was inferred by a preference for exploring the displaced jar compared to the jar that remained in the same location.

Novel Object Recognition

The rat was placed in the box for a 15 min familiarization phase and allowed to explore two identical objects. Following a 3 hr delay period, the rat was returned to the box with two objects (one novel object and a copy of the object from the familiarization phase). Object recognition memory was inferred by a preference for the novel object compared to the familiar object (Broadbent et al., 2010).

Context and Cued Fear Conditioning

Day 1 Conditioning. The rats were placed into the chambers for a 7 min conditioning session that included three tone-shock pairs.

Day 2 Context Test. To assess retention of context fear memory, rats were placed for 8 min into the same chamber used for conditioning, and freezing was measured.

Day 3 Tone Test, Cued. To assess retention of the conditioned fear response to the tone, the rats were placed into a different conditioning chamber and into a different context and received one 10 s tone during an 8 min trial while freezing was measured.

REFERENCES

Broadbent, N.J., Squire, L.R., and Clark, R.E. (2004). Spatial memory, recognition memory, and the hippocampus. Proc. Natl. Acad. Sci. USA *101*, 14515–14520.

Broadbent, N.J., Squire, L.R., and Clark, R.E. (2010). Sustained dorsal hippocampal activity is not obligatory for either the maintenance or retrieval of long-term spatial memory. Hippocampus *20*, 1366–1375.

Brun, V.H., Leutgeb, S., Wu, H.Q., Schwarcz, R., Witter, M.P., Moser, E.I., and Moser, M.B. (2008). Impaired spatial representation in CA1 after lesion of direct input from entorhinal cortex. Neuron *57*, 290–302.

Clark, R.E., Broadbent, N.J., and Squire, L.R. (2005). Hippocampus and remote spatial memory in rats. Hippocampus *15*, 260–272.

Deshmukh, S.S., and Knierim, J.J. (2011). Representation of non-spatial and spatial information in the lateral entorhinal cortex. Front. Behav. Neurosci. *5*, 69.

Deshmukh, S.S., Johnson, J.L., and Knierim, J.J. (2012). Perirhinal cortex represents nonspatial, but not spatial, information in rats foraging in the presence of objects: comparison with lateral entorhinal cortex. Hippocampus *22*, 2045–2058.

Eichenbaum, H., Sauvage, M., Fortin, N., Komorowski, R., and Lipton, P. (2012). Towards a functional organization of episodic memory in the medial temporal lobe. Neurosci. Biobehav. Rev. *36*, 1597–1608.

Fyhn, M., Molden, S., Witter, M.P., Moser, E.I., and Moser, M.B. (2004). Spatial representation in the entorhinal cortex. Science *305*, 1258–1264.

Hafting, T., Fyhn, M., Molden, S., Moser, M.B., and Moser, E.I. (2005). Microstructure of a spatial map in the entorhinal cortex. Nature *436*, 801–806.

Hargreaves, E.L., Rao, G., Lee, I., and Knierim, J.J. (2005). Major dissociation between medial and lateral entorhinal input to dorsal hippocampus. Science *308*, 1792–1794.

Jeffery, K.J., Gilbert, A., Burton, S., and Strudwick, A. (2003). Preserved performance in a hippocampal-dependent spatial task despite complete place cell remapping. Hippocampus *13*, 175–189.

Knierim, J.J., Lee, I., and Hargreaves, E.L. (2006). Hippocampal place cells: parallel input streams, subregional processing, and implications for episodic memory. Hippocampus *16*, 755–764.

Koenig, J., Linder, A.N., Leutgeb, J.K., and Leutgeb, S. (2011). The spatial periodicity of grid cells is not sustained during reduced theta oscillations. Science *332*, 592–595.

Krupic, J., Burgess, N., and O'Keefe, J. (2012). Neural representations of location composed of spatially periodic bands. Science *337*, 853–857.

McClelland, J.L., McNaughton, B.L., and O'Reilly, R.C. (1995). Why there are complementary learning systems in the hippocampus and neocortex: insights from the successes and failures of connectionist models of learning and memory. Psychol. Rev. *102*, 419–457.

Miller, V.M., and Best, P.J. (1980). Spatial correlates of hippocampal unit activity are altered by lesions of the fornix and endorhinal cortex. Brain Res. *194*, 311–323.

Morris, R.G., Schenk, F., Tweedie, F., and Jarrard, L.E. (1990). Ibotenate lesions of hippocampus and/or subiculum: dissociating components of allocentric spatial learning. Eur. J. Neurosci. *2*, 1016–1028.

Mumby, D.G., Gaskin, S., Glenn, M.J., Schramek, T.E., and Lehmann, H. (2002). Hippocampal damage and exploratory preferences in rats: memory for objects, places, and contexts. Learn. Mem. *9*, 49–57.

Navawongse, R., and Eichenbaum, H. (2013). Distinct pathways for rule-based retrieval and spatial mapping of memory representations in hippocampal neurons. J. Neurosci. *33*, 1002–1013.

Parron, C., Poucet, B., and Save, E. (2004). Entorhinal cortex lesions impair the use of distal but not proximal landmarks during place navigation in the rat. Behav. Brain Res. *154*, 345–352.

Sanders, M.J., and Fanselow, M.S. (2003). Pre-training prevents context fear conditioning deficits produced by hippocampal NMDA receptor blockade. Neurobiol. Learn. Mem. *80*, 123–129.

Sargolini, F., Fyhn, M., Hafting, T., McNaughton, B.L., Witter, M.P., Moser, M.B., and Moser, E.I. (2006). Conjunctive representation of position, direction, and velocity in entorhinal cortex. Science *312*, 758–762.

Sauvage, M.M., Beer, Z., Ekovich, M., Ho, L., and Eichenbaum, H. (2010). The caudal medial entorhinal cortex: a selective role in recollection-based recognition memory. J. Neurosci. *30*, 15695–15699.

Solstad, T., Boccara, C.N., Kropff, E., Moser, M.B., and Moser, E.I. (2008). Representation of geometric borders in the entorhinal cortex. Science *322*, 1865–1868.

Squire, L.R., and Alvarez, P. (1995). Retrograde amnesia and memory consolidation: a neurobiological perspective. Curr. Opin. Neurobiol. *5*, 169–177.

Steffenach, H.A., Witter, M., Moser, M.B., and Moser, E.I. (2005). Spatial memory in the rat requires the dorsolateral band of the entorhinal cortex. Neuron *45*, 301–313.

Tsao, A., Moser, M.B., and Moser, E.I. (2013). Traces of experience in the lateral entorhinal cortex. Curr. Biol. *23*, 399–405.

Van Cauter, T., Poucet, B., and Save, E. (2008). Delay-dependent involvement of the rat entorhinal cortex in habituation to a novel environment. Neurobiol. Learn. Mem. *90*, 192–199.

Van Cauter, T., Camon, J., Alvernhe, A., Elduayen, C., Sargolini, F., and Save, E. (2013). Distinct roles of medial and lateral entorhinal cortex in spatial cognition. Cereb. Cortex *23*, 451–459.

Witter, M.P., and Amaral, D.G. (1991). Entorhinal cortex of the monkey: V. Projections to the dentate gyrus, hippocampus, and subicular complex. J. Comp. Neurol. *307*, 437–459.

Witter, M.P., Van Hoesen, G.W., and Amaral, D.G. (1989). Topographical organization of the entorhinal projection to the dentate gyrus of the monkey. J. Neurosci. *9*, 216–228.

Witter, M.P., Naber, P.A., van Haeften, T., Machielsen, W.C., Rombouts, S.A., Barkhof, F., Scheltens, P., and Lopes da Silva, F.H. (2000). Cortico-hippocampal communication by way of parallel parahippocampal-subicular pathways. Hippocampus *10*, 398–410.

Yasuda, M., and Mayford, M.R. (2006). CaMKII activation in the entorhinal cortex disrupts previously encoded spatial memory. Neuron *50*, 309–318.

Zhang, S.J., Ye, J., Miao, C., Tsao, A., Cerniauskas, I., Ledergerber, D., Moser, M.B., and Moser, E.I. (2013). Optogenetic dissection of entorhinal-hippocampal functional connectivity. Science *340*, 1232627. http://dx.doi.org/10.1126/science/1232627.

Medial Entorhinal Cortex Lesions

Only Partially Disrupt Hippocampal Place Cells

and Hippocampus-Dependent Place Memory

Jena B. Hales, Magdalene I. Schlesiger, Jill K. Leutgeb, Larry R. Squire, Stefan Leutgeb, and Robert E. Clark

SUPPLEMENTAL DATA

Degree of retained place cell spatial firing was not predicted small amount of MEC sparing

Because of the large lesion extent, we did not expect that the small fraction of retained tissue could be used to predict place field quality. Accordingly, we did not find any relation between the quality of the place fields and the small amount of spared tissue in either the entire MEC (place field size: r = 0.18, n.s.; spatial information: r = -0.13, n.s.) or in any of the MEC layers. Hippocampal spatial firing in animals with minor MEC sparing was thus equally disrupted as in animals with near-complete MEC lesions (see Figure S2).

Behavioral impairment in the watermaze was independent of delay intervals

Another feature of hippocampal recordings was that the consistency of hippocampal firing was disproportionately impaired in the MEC group relative to the CON group at long intervals between sessions relative to short intervals. We explored whether this finding might be associated with a more pronounced memory deficit after longer compared to shorter retention intervals by performing probe trials at four delays (1 min, 20 min, 90 min, and 6 h) during the second week of watermaze training. After MEC lesions, the behavioral impairment was not exacerbated at longer delay intervals relative to shorter delay intervals (Figure S4). However, there was greater than chance stability in the place fields at intervals of up to 1 day (see Figure 2D) and sparing of memory even at intervals of 1 day in the MEC group (see Figure 3). The remaining level of hippocampal function may thus have been sufficient to partially support behavior at all tested intervals or an alternate, slower learning brain system was beginning to support behavior.

Longer latencies and swim path distances in the watermaze for all lesion groups relative to controls remained throughout the three weeks of testing

All three lesion groups had longer latencies to locate the hidden platform during the first week of training trials (repeated-measures ANOVA for group: $F_{(3)} = 8.05$, $p < 0.001$). This impairment persisted throughout all 15 days

1

of testing. Average latencies during the third week of testing (days 11-15) were longer for all lesion groups relative to controls. The average latency to the platform for CON rats (4.97 ± 0.17 s) was shorter than that of H rats (5.91 ± 0.27 s; $t_{(26)} = 2.93$, $p < 0.01$), MEC rats (7.39 ± 0.48 s; $t_{(26)} = 6.01$, $p < 0.0001$), and MEC+H rats (8.96 ± 0.63 s; $t_{(26)} = 8.37$, $p < 0.0001$). H rats also had a shorter latency than MEC+H rats ($t_{(14)} = 4.44$, $p < 0.001$) and MEC rats ($t_{(14)} = 2.70$, $p < 0.05$), while MEC rats had an average latency that was not different from MEC+H rats ($t_{(14)} = 1.99$, $p = 0.07$). Since latencies can be confounded by swim speed, we also calculated the swim path distances for each training trial. All three lesion groups had longer swim path distances to locate the hidden platform during the first week of training trials (repeated-measures ANOVA for group: $F_{(3)} = 10.57$, $p < 0.0001$). This impairment persisted throughout all 15 days of testing (see Figure 3C). Average swim path distances during the third week of testing (days 11-15) were longer for all lesion groups relative to controls. The average swim path distance to the platform for CON rats (116.49 ± 3.08 cm) was shorter than that of H rats (138.75 ± 6.55 cm; $t_{(26)} = 3.50$, $p < 0.01$), MEC rats (148.76 ± 11.80 cm; $t_{(26)} = 3.68$, $p < 0.01$), and MEC+H rats (170.04 ± 9.64 cm; $t_{(26)} = 6.95$, $p < 0.0001$). H rats also had a shorter distance than MEC+H rats ($t_{(14)} = 2.68$, $p < 0.05$), while MEC rats had an average path distance that was not different from MEC+H rats ($t_{(14)} = 1.40$, $p > 0.1$) or H rats ($t_{(14)} = 0.74$, $p > 0.1$).

Unshocked control comparison group for context fear conditioning

Both the MEC and CON groups exhibited more freezing than unshocked controls on the context and cued (tone) tests, demonstrating significant fear memory retention (unshocked control means did not differ from zero; MEC versus unshocked for context: $t_{(14)} = 4.19$, $p < 0.001$; CON versus unshocked $t_{(14)} = 3.18$, $p < 0.01$; MEC versus unshocked for tone: $t_{(14)} = 5.26$, $p < 0.01$; CON versus unshocked $t_{(14)} = 7.45$, $p < 0.001$).

SUPPLEMENTAL FIGURE LEGENDS

Figure S1. MEC lesions were nearly complete, in particular in the superficial layers, related to Figure 1.

(A) Average lesion size in rats used for electrophysiological recordings (P; $n = 5$) and in rats used for behavioral experiments (B; $n = 14$). Layer II (blue), layer III (red), and deep layers (V/VI, black) were quantified separately. Error bars represent SEM.

(B) Percentage of lesioned tissue for behavioral rats with representative large (Rat 3039) and average (Rat 2983) MEC lesions and for all five rats with hippocampal recordings. L and R correspond to left and right hemisphere, respectively. No successful recordings were obtained from the two hemispheres shaded in grey.

(C) Detailed illustration of complete series of sagittal sections. The colored boxes identify corresponding hemispheres in (B) and (C).

(D) Amount of MEC tissue in control (left) and MEC (middle) groups and % spared tissue (right). Spared tissue was measured for each section throughout the mediolateral extent of the MEC. Each cell layer in rats used for behavior **(top)** and electrophysiology **(bottom)** is shown separately. In the tissue of four hemispheres from three animals with electrophysiological recordings, we observed MEC layer III neurons that showed signs of substantial damage in addition to tissue in which neurons were completely ablated. For these animals, the MEC volume with any stained neurons is shown as red squares and MEC volume with only cells of normal appearance is shown as purple circles. The more conservative estimate that included only tissue without neurons was used in all quantitative analyses, including the calculation of the mean lesion size.

$*p < 0.001$

Figure S2. The degree of retained spatial firing of hippocampal place cells was not predicted by the small amount of spared tissue in MEC layer III or deep layers, and larger place fields were seen throughout the entire series of six 10-min recording sessions within a day, related to Figure 2.

(A, B) The spatial firing in the MEC group was disrupted, but not completely abolished (see Figure 2). Changes in place field size and spatial information were unrelated to the extent of spared tissue in layer III and in the deep

layers (V/VI) of the MEC (all r values are n.s.). The mean of the cells that were recorded in each hemisphere is plotted against the ipsilateral lesion size (n = 8 hemispheres with recordings in five rats). Lesions in layer II of all hemispheres were > 97 % complete, and correlation analysis was not performed because of the small degree of remaining variability.

(C) The firing rate (including cells that were active in rest and/or behavior) in the MEC group was also unrelated to the extent of tissue damage in each hemisphere. There was no group difference in firing rate after excluding silent cells and correlation analysis was therefore not performed on these data.

(D) Example cells from two control and from two MEC rats with large lesions. For the lesioned rats, cells that were recorded from the left and right hemisphere on the same day are shown. The colored boxes depict hemispheres for which detailed histology is shown with corresponding colors in Figure S1. For each cell, the depicted 10-min session is the most representative for the day (i.e., closest to the mean field size of the recording sessions of the day). The spatial firing patterns of each cell is shown as the trajectory (grey) with superimposed spike locations (red dots) on the left of each panel and as color-coded heat maps on the right of each panel. In the heat maps, pixels at the peak firing rate are in red and pixels with no firing are in dark blue. Note that data for Rat 505 were recorded from a square arena. There was substantial variability in the quality of spatial firing between cells that were simultaneously recorded within a recording session, and decreased place cell quality was observed irrespective of the amount of remaining tissue in MEC rats (see A-C). For example, the layer III lesion in the left hemisphere of rat 434 was > 97 % complete, and the spatial firing of cells was of comparable quality to that of rat 514 in which the lesion in both hemispheres was 88 % complete. Error bars represent SEM.

(E) Field size distribution for MEC and CON groups.

(F) Examples of firing fields throughout a series of 10-min sessions within a day. Color-coded rate maps depict the spatial distribution of firing in the recording enclosure during each 10-min session. The peak rate (red) is scaled to the maximum for the six sessions. Intervals between sessions were 2 min, 20 min, and 6 h. Each row illustrates a cell. Note that data for MEC lesion Cell 1 and Cell 2 were recorded from a square arena.

(G-J) The firing characteristics of hippocampal cells in the control and in the MEC group are shown separately for each of the six 10-min foraging sessions of a day (mean ± SEM). The mean firing rate (G, all cells that were

active during behavior and/or during rest periods) in the MEC group increased during the course of the six daily sessions (Kruskal-Wallis test, df = 5, $p < 0.001$ with $p < 0.05$ for the 1st versus 2nd, 1st versus 3rd, and 1st versus 4th session), but did not reach control levels (Mann-Whitney U test for session 4, which is the session with the smallest difference: $p < 0.01$). The firing rate of active cells (H), the place fields size (I), the spatial information (J), and the spatial coherence (K) did not change over the course of the six daily sessions (Kruskal-Wallis test, all p values > 0.05).

Figure S3. Behavioral impairment in the watermaze following MEC lesion was independent of delay intervals, related to Figure 3.

(A) Mean path reconstruction error versus the number of cells used in the reconstruction indicates a decrease in spatial firing quality in MEC rats compared to controls.

(B) Probe trial performance during the second week of watermaze training with mixed delay intervals between training and probe trials in rats with lesions of the hippocampus (H, $n = 8$), lesions of the medial entorhinal cortex (MEC, $n = 8$), lesions of both structures (MEC+H, $n = 8$) and sham lesions (CON, $n = 20$). The scores represent the percentage of time each group spent in the small zone centered on the trained platform location (left) or in the training quadrant (right) the during a 60-s probe trial performed 1 min, 20 min, 90 min, or 6 h after the last training trial of the day. *Small zone measure:* The CON group showed declining performance at longer intervals (1 min versus 6 h: $t_{(19)} = 6.21$, $p < 0.0001$). All three lesion groups were impaired at the short 1-min and 20-min intervals, and the H and MEC+H groups were also impaired at the 90-min interval relative to the CON group (1 min, MEC+H: $t_{(26)} = 3.17$, $p < 0.01$; 1 min, MEC: $t_{(26)} = 2.92$, $p < 0.01$; 1 min, H-: $t_{(26)} = 2.52$, $p < 0.05$; 20 min, MEC+H: $t_{(26)} = 4.22$, $p < 0.001$; 20 min, MEC: $t_{(26)} = 3.94$, $p < 0.001$; 20 min, H: $t_{(26)} = 2.15$, $p < 0.05$; 90 min, MEC+H: $t_{(26)} = 2.80$, $p < 0.01$; 90 min, H: $t_{(26)} = 2.40$, $p < 0.05$). We therefore found impaired performance in all lesion groups at shorter intervals (1 min and 20 min) and not at longer intervals (6 h). *Quadrant measure:* The CON group showed declining performance at longer intervals (1 min versus 6 h: $t_{(19)} = 9.76$, $p < 0.0001$), and the MEC and H groups performed similarly to controls. The MEC+H group was impaired at the shorter intervals but not at the longer intervals (1 min: $t_{(26)} = 2.44$, $p < 0.05$; 20 min: $t_{(26)} = 3.55$, $p < 0.01$). Taken together, the

impairment of all three lesion groups at shorter but not at longer intervals reflected the poorer performance in the CON group at longer intervals and not necessarily a selective impairment of the lesion groups at short intervals. Furthermore, the lack of impairment at the longer (i.e., 6 h) interval is consistent with the emerging recovery at the 1day interval during week 2 (see Figure 3). Even though the flat behavioral performance across different retention intervals after MEC lesions did not correspond closely to the decreasing place field stability at longer intervals, it may be sufficient for intact behavioral performance that place cell stability is higher than chance at all of the tested intervals.

A

B Behavior / Physiology

MEC II MEC III MEC V/VI

Rat 3039 Rat 2983 Rat 405 Rat 434 Rat 502 Rat 514 Rat 587

◇ MEC II □ MEC III △ MEC V/VI

C

Control

MEC Lesion Behavior Rat 3039

MEC Lesion Behavior Rat 2983

MEC Lesion Physiology Rat 405

MEC Lesion Physiology Rat 434

MEC Lesion Physiology Rat 514

Lateral → Medial

D Control Behavior MEC lesion MEC lesion / Control

E Control Electrophysiology MEC lesion MEC lesion / Control

◇ MEC II □ MEC III ○ MEC III (excluding damaged cells) △ MEC V/VI
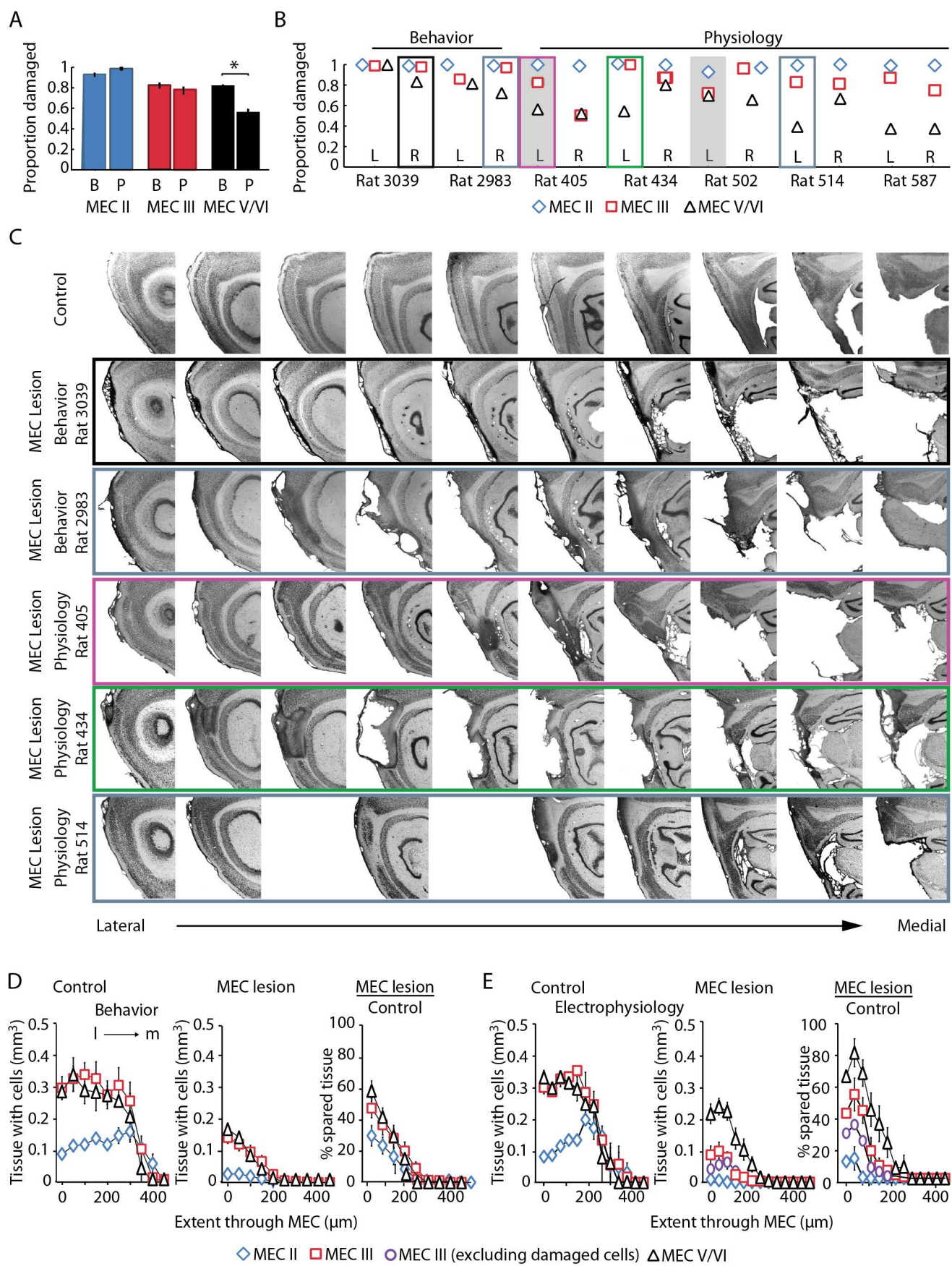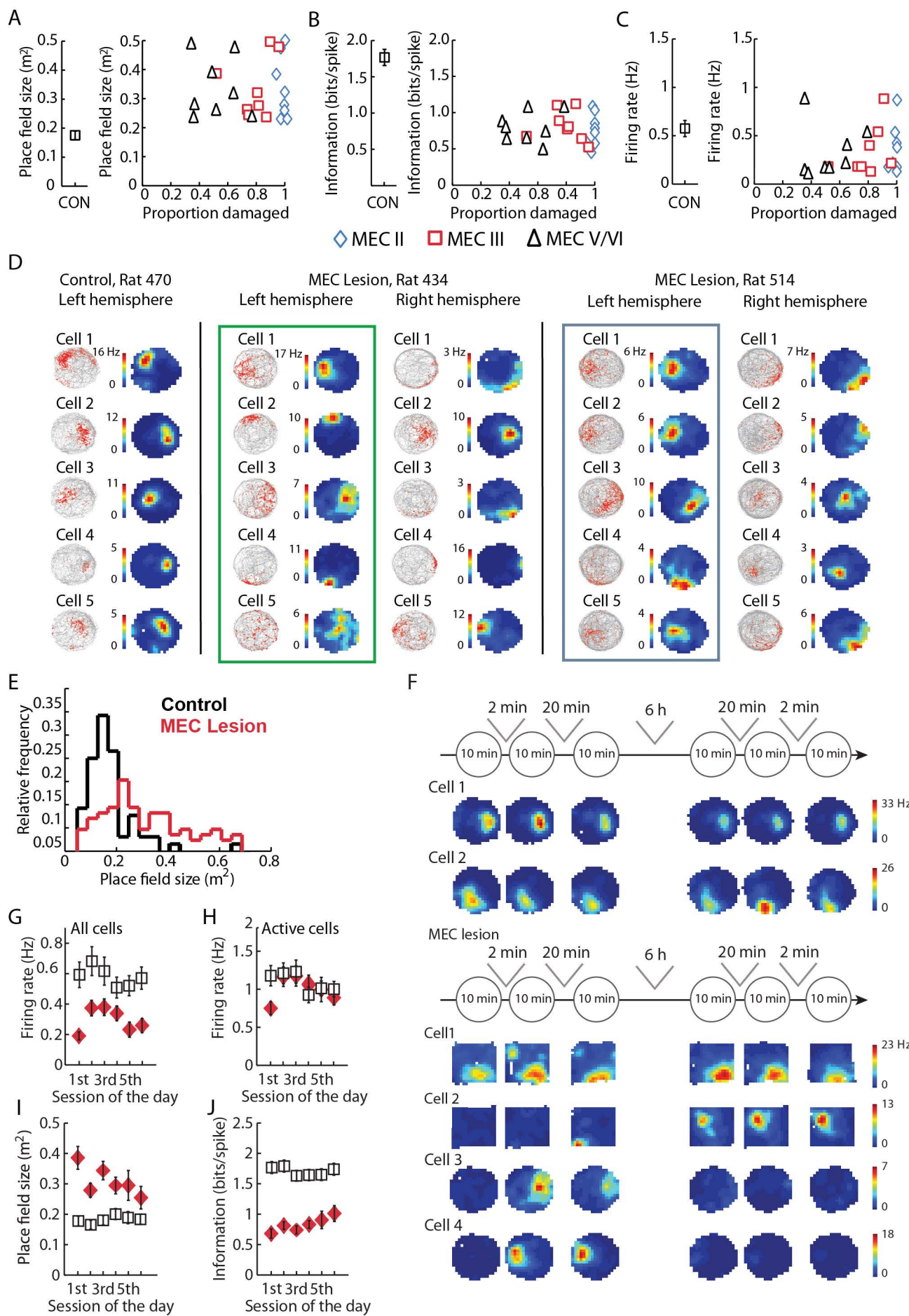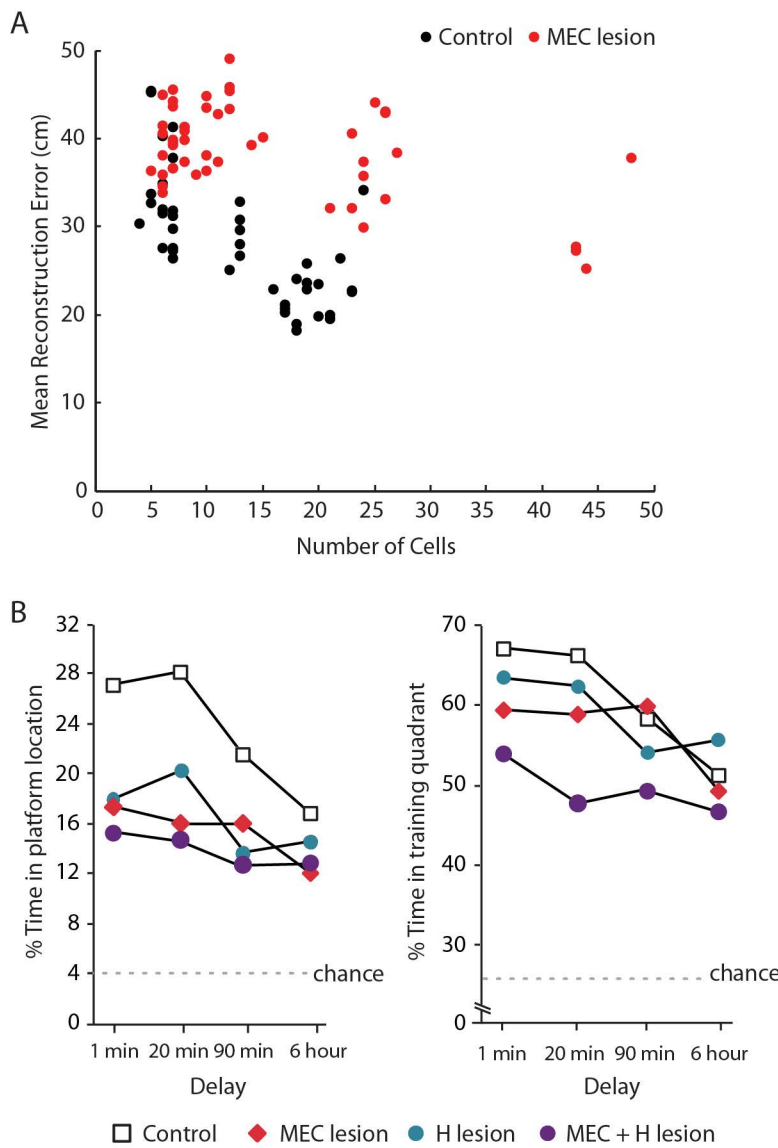
Figure S3, Relates to Figure 2

Figure S3, Relates to Figure 3

SUPPLEMENTAL EXPERIMENTAL PROCEDURES

Surgery

For the hippocampal (H) group, IBO was injected into 18 sites (as in Clark et al., 2000). For the MEC group, NMDA was injected into 8 sites bilaterally along the entire dorsoventral axis of the MEC. The needle was lowered along a single track at ML ±4.6 mm with the needle tip placed immediately anterior to the transverse sinus (the AP coordinate) and pointed anterior at an angle of 22°. For the MEC+H group, the procedures that were used for each lesion alone were combined.

Electrophysiological recordings

Apparatus and pretraining. A black square enclosure (1 m x 1 m, 50 cm walls, white cue card) was placed in the center of a room. The enclosure contained a polarizing cue card (20 cm x 50 cm), remained at a constant location within the room, and was surrounded by constant background cues. No curtains were used. Rats were trained to forage for randomly scattered cereal crumbs in the enclosure for 5 days in two daily 10-min sessions.

Recording procedures. After surgery, tetrodes were slowly advanced into the CA1 area of the hippocampus. As expected (Bragin et al., 1995a, b), sharp wave ripples were not diminished by the MEC lesion and were used to guide electrode advancement into the cell layer in all rats. During tetrode advancement and during recordings, the electrode assembly was connected to a multichannel, impedance matching, unity gain preamplifier headstage. The output was routed to a data acquisition system with 64 digitally programmable differential amplifiers (Neuralynx, Tucson, AZ, USA). Spike waveforms above a threshold of 40-45 µV were time-stamped and digitized at 32 kHz for 1 ms. The rat's position was tracked at 30 Hz by recording the position of light-emitting diodes that were placed above the head. Local field potentials were acquired by recording one channel of each tetrode with the filters set to the 1-450 Hz band.

After recovery from surgery, training continued in a different room than during pretraining. The second room contained a black circular enclosure (1 m diameter, 50 cm walls, 20 cm wide x 50 cm high, white cue card), and rats were trained for 7-10 days to randomly forage for up to six 10-min sessions per day. Between sessions, rats rested for two min or 20 min in a transparent holding chamber placed adjacent to the behavioral apparatus or for 6 h in a holding area within the laboratory. Recordings during random foraging in this experimental design began when tetrodes were positioned in the CA1 cell layer and when the rats ran continuously over the entire box surface throughout each 10-min random foraging session. For intersession-intervals of 1 day, recordings from the same cells were compared between sessions on 2 consecutive days. To obtain additional data to assess firing rates during resting and recording stability, we also recorded spikes and local field potentials while the rat was in a holding box for 10 min at the beginning and for 20 min at the end of each recording day. After up to 4 days of recordings in the room in which training began after surgery, one day of recordings was performed in the room in which pretraining was performed before surgery. These recordings showed comparable results to the recordings in the room in which training began after surgery and are not presented because they are of lesser relevance to the memory testing, which was performed in rooms that the rats were not familiarized with before the lesion surgery. On the last recording day, rats were placed in a novel room containing a white square enclosure (1 m x 1 m, 50 cm walls, black cue card) and trained for three 10-min sessions.

Data Analysis

Spike sorting and cell tracking. Spike sorting was performed off-line using customized cluster-cutting software (MClust, D. Redish) with modifications (Mankin et al., 2012). Recordings during rest periods throughout the day were used to confirm recording stability during the experiment and to identify hippocampal cells that were silent or fired at low rates during behavior. Clustering was performed manually in two-dimensional projections of the multidimensional parameter space (consisting of waveform amplitudes, waveform energies, and the peak-to-valley difference) using autocorrelation and cross-correlation functions as additional separation tools and separation criteria. Putative excitatory cells were distinguished from putative inhibitory interneurons by spike width and average rate. Putative interneurons were not included in the analysis.

Rate maps. The recording enclosure was divided into 5 cm x 5 cm pixels. Spatial firing rate distributions were constructed by summing the total number of spikes that occurred in each location bin, dividing by the amount of time that the animal spent in that location, and then smoothing with a box car filter (Koenig et al., 2011). The rate maps were used to determine the place field size, the spatial information, and the spatial coherence within each 10-min recording session.

Spatial correlation. The spatial similarity of place fields across two conditions was calculated using Pearson's correlation. The correlation coefficient was calculated by comparing the firing rates between all pixels at corresponding locations. Sampling errors for cells with low firing rates were minimized by excluding cells with fewer than 150 spikes during the 600-s recording interval. For each comparison, cells had to exceed a mean firing rate threshold of 0.25 Hz in the first condition to be included in the analysis.

Spatial information. The information score describes the information density per spike and was calculated as described by Skaggs et al. (1996), using the following formula:

$$I = \sum_{i=1}^{N} p_i \frac{\lambda_i}{\lambda} \log_2 \frac{\lambda_i}{\lambda}$$

where I is the information density measured in bits per spike, i is the index of the pixels of the place field, p_i is the probability of the rat being at location i, λ_i is the average firing rate of the cell when the rat is at location i, and λ is the total average firing rate.

Spatial coherence. The first order spatial autocorrelation of each place field map was calculated in order to estimate the extent to which the firing rate in a pixel was predicted by the firing rates in the neighboring pixels (Muller and Kubie, 1989).

Place field size. To determine the place field size, we recalculated the firing rate in each 5 cm x 5 cm pixel by applying an adaptive smoothing method, which expands a circle around each pixel until

$$r \geq \frac{a_i}{n\sqrt{s}}$$

where r is the radius of the circle in bins, n is the number of occupancy samples within the circle, s is the total

number of spikes in those occupancy samples and the constant $\pm$ is set to 10,000. Using the adaptive map, the place field size was calculated by identifying the pixel with the peak firing rate and by then extending the field to any adjacent pixels that exceeded 20 % of the peak rate. The area that was covered by these pixels was the field size. Fields with a size of less than 9 pixels (i.e., 225 cm^2) or with a peak rate of less than 1 Hz were considered spurious firing and were excluded from the analysis. A threshold of 0.25 Hz mean firing rate was additionally applied to select active cells.

Path reconstruction. Spatial rate decoding and path reconstruction were performed following the Bayesian method described in (Zhang et al. 1998). Let $\boldsymbol{x}(t) = [x(t)\ y(t)]$ be the position vector of the animal at time t, and let $\boldsymbol{n}(t) = [n_1(t)\ n_2(t) \cdots n_K(t)]$ be the population vector of spike counts from each of K cells within the period $[t - \frac{1}{2}\Delta t, t + \frac{1}{2}\Delta t)$ for some short duration Δt. Further, let $\mathcal{N} = \{\boldsymbol{n_1}, \boldsymbol{n_2}, ..., \boldsymbol{n_P}\}$ and $\mathcal{X} = \{\boldsymbol{x_1}, \boldsymbol{x_2}, ..., \boldsymbol{x_M}\}$ be the respective sets of position and population spike count vectors observed during the decoding period. Then, given that $\boldsymbol{n}(t) = \boldsymbol{n_i}$, the probability that $\boldsymbol{x}(t) = \boldsymbol{x_j}$, is given by

$$P(\boldsymbol{x_j}|\boldsymbol{n_i}) = \frac{P(\boldsymbol{n_i}|\boldsymbol{x_j})P(\boldsymbol{x_j})}{P(\boldsymbol{n_i})}$$

where $P(\boldsymbol{x_j})$ is the probability of finding the animal in the pixel associated with $\boldsymbol{x_j}$, and $P(\boldsymbol{n_i}) = \sum_m P(\boldsymbol{n_i}|\boldsymbol{x_m})$ is the probability of observing the population spike count vector $\boldsymbol{n_i}$. Under the simplifying assumption that the firing rates of the individual cells are independent and follow an inhomogeneous Poisson process, the prior probabilities are obtained by

$$P(\boldsymbol{n_i}|\boldsymbol{x_j}) = \prod_{k=1}^{K} \frac{\left(\lambda_k(\boldsymbol{x_j})\Delta t\right)^{n_{ik}}}{n_{ik}!} \exp(-\lambda_k(\boldsymbol{x_j})\Delta t)$$

where $\lambda_k(\boldsymbol{x_j})$ is the pixel rate of the kth cell associated with the position $\boldsymbol{x_j}$.

Since the $\lambda_k(\boldsymbol{x_j})$ and $P(\boldsymbol{x_j})$ are presumed constant over the period of decoding and reconstruction, these were determined using data from the entire 10 minute recording session (see "Rate maps" and "Spatial information"). $\mathcal{N}$ and $\mathcal{X}$ were determined using data from the first 5 minutes of each recording session only. Path reconstruction

was performed only on the latter 5 minutes of each session. To each $\boldsymbol{n}(t)$ in the latter half-session, we assigned

the $\boldsymbol{n}_i \in \mathcal{N}$ such that $\boldsymbol{n}_i = \mathrm{argmin}_{\boldsymbol{n}_p} \|\boldsymbol{n}(t) - \boldsymbol{n}_p\|$. If $\boldsymbol{n}_i \neq \boldsymbol{0}$, the reconstructed position vector $\tilde{\boldsymbol{x}}(t)$ was

assigned an $\boldsymbol{x}_j \in \mathcal{X}$ with probability $P(\boldsymbol{x}_j | \boldsymbol{n}_i)$. Otherwise, the previous reconstructed position was used. A Δt of

1 second was used in both the decoding and reconstruction stages.

Behavioral Testing

Morris watermaze. Testing was conducted in a standard watermaze (1.8 m diameter) with a video tracking system

(San Diego Instruments). The platform (12.7 cm diameter) could be raised or lowered remotely. This allowed

memory to be assessed with reinforced probe trials during all phases of training. After finding the platform, the

rats remained on the platform for 30 s. *Three-week protocol.* For the first week of testing (Week 1; M-F), rats

were given one reinforced probe trial followed by four training trials (i.e., acquisition). For Week 2, rats were

given a single standard training day followed by 4 days, as before, except they also received a single additional

reinforced probe trial after completion of the last daily training trial. These additional probe trials were scheduled

1 min, 20 min, 90 min, or 6 h following the final training trial of the day. The order of these additional probe trial

delays was counterbalanced. In week 3 the rats were given an additional 5 standard training days.

Displaced object recognition, DOR. Displaced object recognition testing was conducted in a circular, opaque

apparatus (103-cm diameter) with four distinct graphics on the wall, one in each quadrant. A video camera

recorded each rat's exploratory behavior. Jar exploration was scored by an experimenter blind to group

membership (Clark et al., 2000). Spatial recognition memory was inferred by a preference for exploring the

displaced jar compared to the jar that remained in the same location.

Novel object recognition, NOR. Testing was conducted in a box measuring 35 cm x 41.5 cm x 50 cm. Stimuli

consisted of ceramic or plastic objects that varied in color and size. The procedure was repeated 10 to 13 days later

with a new set of objects, and the scores were averaged. Object recognition memory was inferred by a preference for the novel object compared to the familiar object.

Context and Cued fear conditioning. Rats were tested in a sound attenuating fear-conditioning chamber (MED-Associates, Burlington, VT). Scrambled foot shock (1 mA; 2 s) was delivered through the floor's steel rods. A 10-s pure tone (90 dB) was delivered to co-terminate with the foot shock. *Day 1 Conditioning.* The rats were placed into the chambers for a 7-min conditioning session, during which there were 3 min of quiet followed by three tone–shock pairs (separated by at least 60 s). *Day 2 Context Test.* To assess retention of context fear memory, rats were placed for 8 min into the same chamber used for conditioning, and freezing was measured. *Day 3 Tone Test (cued).* To assess retention of the conditioned fear response to the tone, the rats were placed into a different conditioning chamber and into a different context (the context was changed by inserting a triangular façade and a plastic floor to cover the steel shock rods). After a 4-min baseline period, the rats received one 10-s tone and remained in the chamber for the remainder of the 8-min trial while freezing was measured.

Neurohistological methods

Rats were administered an overdose of sodium pentobarbital and perfused transcardially with buffered 0.9 % NaCl solution followed by either 4 % or 10 % formaldehyde solution (in 0.1 M phosphate buffer). Brains were then removed from the skull and cryoprotected in a solution of 20 % glycerol and 10 % formaldehyde or kept in a solution of 4 % formaldehyde followed by 30 % sucrose. For the H and some of the CON ($n = 8$) rats, coronal sections (50 µm) were cut with a freezing microtome beginning just anterior to the hippocampus and continuing caudally through the length of the hippocampal region. One in every five sections was mounted and stained with cresyl violet. For the MEC-lesioned, MEC+H-lesioned, and the remainder of the CON rats ($n = 23$), sagittal sections (40 or 50 µm) were cut with a freezing microtome beginning just lateral to the hippocampus and continuing medially through the hippocampal region for each hemisphere. For the rats used for physiological recordings ($n = 5$ MEC, $n = 3$ CON), every 2nd section was mounted and stained with cresyl violet. For the

MEC+H rats ($n = 8$) and some of the CON rats ($n = 4$), every 4th section was mounted and stained with cresyl violet, and for the MEC and remaining CON rats ($n = 16$), every 3rd section was mounted and stained with cresyl violet. The cresyl violet stained sections were used for an initial assessment of the lesion size and, in recording animals, to determine the tetrode locations across the series of sections through the hippocampus. An angular deviation between the plane of sectioning and the electrode tracks resulted in an apparent shift of the tissue damage between sections. The electrode tip was considered to be located in the section where the tissue damage was most ventral. Recordings from a tetrode were included in the data analysis if the tetrode's final position was in the CA1 pyramidal cell layer.

For each of the lesion animals and for 10 CON animals, additional series of sectioned brains were prepared for immunolocalization of neuron-specific nuclear protein (NeuN) by using an anti-NeuN (1:15,000, Chemicon) monoclonal mouse antibody. The same section intervals that were used for cresyl violet staining were also used for NeuN immunolocalization with the exception of the rats used for physiological recording, for which every 4th section was used. A biotinylated anti-mouse IgG (H+L) (1:1,000, Vector BA-2000) was used as the secondary antibody. We acquired images of the NeuN stained tissue sections using a Leica Microsystems, Inc., DM6000 microscope, and Stereo Investigator (mbf Bioscience; MicroBrightField, CA, USA) was used to analyze images from every other mounted section for all of the stained brains. We calculated the volumes of spared tissue using the Cavalieri method by an overlaid sampling grid with an area per point of 150 µm squared on the tissue image and, on each section, counted the total number of grid points in contact with each of the following anatomical regions: MEC layer II, MEC layer III, MEC deep (V/VI) layers, dorsal parasubiculum, ventral parasubiculum, and hippocampus. The total estimated volume of the spared tissue in each region was calculated by summing the section thickness, the section sampling fraction, and the number of selected grid points per section multiplied by the area associated with each grid point. We then reported the percent damage in each region, which was calculated by dividing the volume of damaged tissue by the average volume of tissue in the CON rats and multiplying by 100. Two rats in the MEC group for behavioral testing were excluded from histological quantification due to poor NeuN staining, but the lesions and behavior of these two animals were

indistinguishable from the rest of the MEC group.

SUPPLEMENTAL REFERENCES

Bragin, A., Jandó, G., Nádasky, Z., Hetke, J., Wise, K., and Buzsáki, G. (1995a). Gamma (40-100 Hz) oscillation in the hippocampus of the behaving rat. J Neurosci 15, 47–60.

Bragin, A., Jandó, G., Nádasky, Z., van Landeghem, M., and Buzsáki, G. (1995b). Dentate EEG spikes and associated interneuronal population bursts in the hippocampal hilar region of the rat. J Neurophysiol 73(4), 1691–1705.

Clark, R.E., Zola, S.M., and Squire, L.R. (2000). Impaired recognition memory in rats after damage to the hippocampus. J. Neurosci. 20, 8853–8860.

Mankin, E.A., Sparks, F.T., Slayyeh, B., Sutherland, R.J., Leutgeb, S., and Leutgeb, J.K. (2012). A neuronal code for extended time in the hippocampus. Proc. Nat. Acad. Sci. U S A 109(47), 19462–19467.

Muller, R.U., and Kubie, J.L. (1989). The firing of hippocampal place cells predicts the future position of freely moving rats. J. Neurosci. 9(12), 4101–4110.

Skaggs, W.E., McNaughton, B.L., Wilson, M.A., and Barnes, C.A. (1996). Theta phase precession in hippocampal neuronal populations and the compression of temporal sequences. Hippocampus 6(2), 149–172.